

## OPTICAL RECOMBINATION LINES AND TEMPERATURE FLUCTUATIONS

X.-W. Liu

University College London

### RESUMEN

Hace tres décadas que Peimbert encontró que las temperaturas del salto de Balmer en regiones H II y planetarias (PNe) son sistemáticamente menores a las obtenidas con las líneas del [O III]. Sugirió que debido a la existencia de fluctuaciones de la temperatura, las abundancias de elementos pesados derivadas de líneas de excitación colisional (CELs) eran sistemáticamente subestimadas. En este trabajo hago una revisión de las determinaciones recientes de elementos pesados en PNe con líneas débiles de elementos pesados (ORLs). En todas las especies iónicas estudiadas, las ORLs dan abundancias mayores que las CELs. El cociente de abundancias ORL a CEL varía de objeto a objeto y está correlacionado con la diferencia de temperaturas del [O III] y del salto de Balmer. Las fluctuaciones de temperatura y densidad solas no pueden explicar las grandes discrepancias en abundancias obtenidas con ORL y CEL en un número pequeño de nebulosas. Se sugiere que estos casos extremos pueden contener regiones ricas en metales similares a las observadas en PN rejuvenecidas, como Abell 30.

### ABSTRACT

Three decades ago, Peimbert found that in H II regions and planetary nebulae (PNe) Balmer jump temperatures are systematically lower than [O III] forbidden line temperatures. He suggested that because there are large temperature fluctuations in nebulae, as a consequence, heavy element abundances derived from collisionally excited lines (CELs) have been systematically underestimated. In this article, I review the recent abundance determinations for PNe using faint heavy element optical recombination lines (ORLs). For all the ionic species studied, ORLs yield higher abundances than CELs. The ratio of ORL to CEL abundances varies from object to object and correlates with the difference between the [O III] and Balmer jump temperatures. Temperature and/or density fluctuations alone are found to be insufficient to explain the very large discrepancies between the ORL and CEL abundances observed in a small number of nebulae. It is suggested that these extreme nebulae may contain metal-rich inclusions similar to those observed in “born-again” PN such as Abell 30.

*Key Words:* **ATOMIC PROCESSES — ISM: ABUNDANCES — PLANETARY NEBULAE**

### 1. INTRODUCTION

Faint nebular lines as potential diagnostics for nebular abundances and physical conditions were first stressed by Wyse (1942), who published deep spectra obtained with I. S. Bowen using the Lick 36-inch reflector for a number of bright PN. He detected about 270 spectral lines, many were permitted transitions from abundant C, N and O ions. In the Saturn Nebula NGC 7009, over twenty O II lines were observed. Wyse argued that these lines must originate from electron captures by  $O^{2+}$  ions, just as the Balmer lines originate from electron captures by  $H^+$  ions, and that therefore the relative intensities of the O II and H I lines should give a measure of the  $O^{2+}/H^+$  abundance ratio. He derived  $O^{2+}/H^+ = 8 \times 10^{-3}$ , compared to  $2 \times 10^{-5}$  deduced by Menzel & Aller (1941) from the [O III] forbidden lines. Early measurements of carbon abundances using C II and C III ORLs were attempted by Aller

& Menzel (1945) and Torres-Peimbert & Peimbert (1977). They found that carbon is strongly overabundant in some PN. Burgess & Seaton (1960) used O III, O IV and O V permitted lines to obtain abundances in NGC 7027 of the ions  $O^{3+}$ ,  $O^{4+}$  and  $O^{5+}$ , which are not represented by optical CELs.

Excited by the same physical mechanism as the hydrogen lines, ionic abundances derived from ORLs have the advantage that they are essentially independent of the thermal and density structure of the nebula under study. On the other hand, they are much weaker than forbidden lines excited by the more efficient collisional process and could be contaminated by excitation mechanisms other than recombination, such as radiative fluorescence (Seaton 1968; Kaler 1972; Grandi 1975, 1976). Thus care must be taken in choosing lines that are suitable for abundance determinations. Strong O III and N III permitted lines observed in high excitation PN are excited by the

Bowen fluorescence mechanism. Some of the O III lines are also enhanced by the charge transfer reaction of  $O^{3+}$  with  $H^0$ , which yields  $O^{2+}$  in excited states (Dalgarno et al. 1981). Thus these lines are not suitable for abundance determinations. Even so,  $O^{3+}/H^+$  abundances can still be obtained by observing lines that cannot be excited by these two processes, such as the  $2p3p\ ^3D-2p3d\ ^3F^o$  multiplet at 3265 Å (Liu & Danziger 1993a).

The launch of the *IUE* made it possible to obtain carbon abundances from CELs observable only in the UV. The results were found to be systematically (but not always) lower than those derived from optical permitted lines (e.g., Harrington et al. 1980; Kaler 1986; Barker 1991 and references therein), thus casting some doubt on the recombination interpretation of those faint optical permitted transitions and their eligibility as reliable abundance indicators. Prior to 1990, abundance determinations using weak heavy element ORLs were hindered by several intertwined difficulties. Even in the best studied case of C II, apart from 3d–4f  $\lambda 4267$ , few lines from other multiplets were observed. It has been known for some time that photographic observations can lead to the intensities of faint lines being overestimated (Miller 1971). The low S/N ratios of faint lines, typical of early observations, also tend to bias the measurements towards higher values (Rola & Stasińska 1994). Finally, little high quality atomic data were available for multi-electron atomic systems. Large observational uncertainties, small numbers of lines observed, coupled with the lack of atomic data, made it difficult to establish the nature of those faint lines.

With the advent of high quantum efficiency, large dynamic range and large format CCDs, it is now possible to obtain high quality measurements of many faint nebular emission lines for bright nebulae. Meanwhile, the completion of the Opacity Project (Seaton 1987; Cunto et al. 1993) has allowed the atomic data necessary to analyze these weak spectral lines, specifically their effective recombination coefficients, to be calculated with high accuracy. Analyses so far confirm that essentially all the weak heavy element permitted transitions detected in PN spectra, including those of C II, N II, O II and Ne II, are of recombination origin and thus yield information about abundances of the recombining ions. In the remaining sections of this article, I will summarize some of the recent results of abundance determinations using heavy element ORLs and discuss the results in the context of the long-debated temperature fluctuations, density inhomogeneities, abundance gradients and their effects on abundance determinations. I will

concentrate on PN. H II regions are addressed in a separate contribution by C. Esteban in this volume. Earlier reviews on the subject are given by Peimbert (1994), Stasińska (1998) and Liu et al. (1999).

## 2. ORL HEAVY ELEMENT ABUNDANCES

Heavy element ORLs typically have an emission equivalent width of a few Å or less, thus medium to high resolution spectroscopy is needed to detect them by suppressing the underlying continuum (nebular plus stellar) and sky background. High resolution is also essential as the lines often blend together at low resolutions. Given that nebular lines typically have a width of 0.5 Å due to nebular expansion, observation with a resolution of  $\sim 1$  Å is optimal and can be achieved with a long-slit spectrograph. Echelle spectrographs offer higher resolutions and thus can be helpful for line identification and deblending. However, compared to long-slit spectrographs, echelle spectrographs generally have a lower throughput, a restricted slit-length, and are more difficult to calibrate and perform sky-subtraction.

In PNe of medium excitation, most C, N, O and Ne are doubly ionized. The 3s–3p, 3p–3d and 3d–4f transition arrays of C II, N II, O II and Ne II fall in the optical region, and thus they are the most easily observed. N II, O II and Ne II all have a rich spectrum. With a single valence electron, C II emission is concentrated in a few lines and C II  $\lambda 4267$  is often the strongest heavy element ORL seen in a PN spectrum. Sample spectra showing the rich ORLs detected in two Galactic bulge PN are plotted in Figure 1. The strongest transitions from the 3d–4f array of C II, N II, O II and Ne II are marked. Although weaker than the strongest 3s–3p and 3p–3d lines, the emissivities of the 3d–4f lines are insensitive to optical depth effects, and, being very hydrogenic, their effective recombination coefficients can be calculated to a high accuracy, although care must be taken to allow for effects caused by the breakdown of *LS*-coupling (Liu et al. 1995). The 3d–4f lines are extremely unlikely to be contaminated by fluorescence excitation. The four transitions marked in Figure 1 have the further advantage that, being the transitions with the highest total angular momentum quantum number  $J$  amongst the whole 3d–4f array (and the strongest), their emissivities are independent of the coupling scheme, making them particularly reliable for abundance determinations.

The abundance of recombining ions relative to  $H^+$  is given by

$$\frac{X^{+i+1}}{H^+} = \left[ \frac{\lambda(\text{Å})}{4861} \right] \times \left[ \frac{\alpha_{\text{eff}}(H\beta)}{\alpha_{\text{eff}}(X^{+i}, \lambda)} \right] \times \left[ \frac{I(X^{+i}, \lambda)}{I(H\beta)} \right],$$

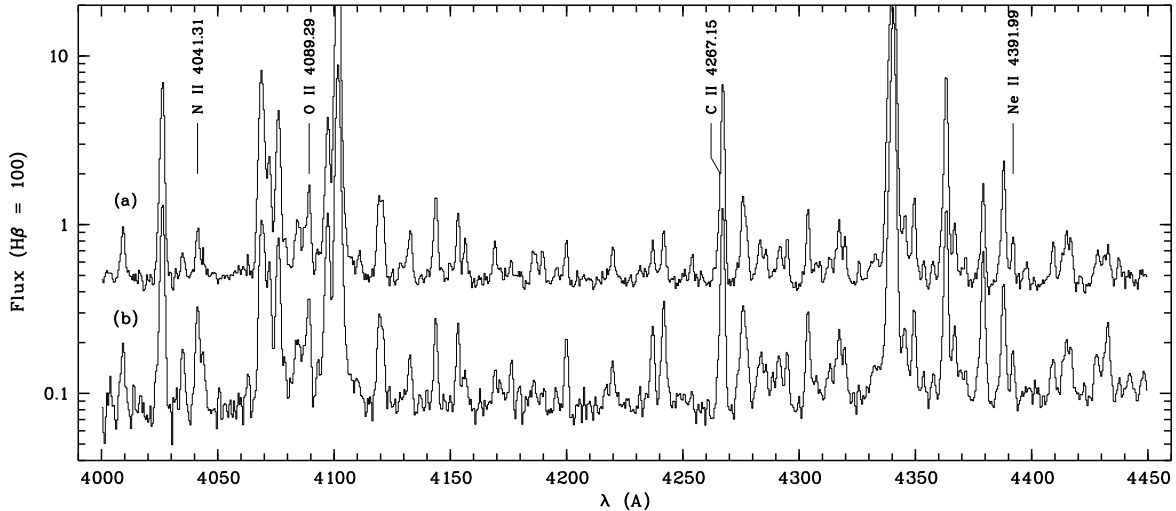


Fig. 1. Sample spectra of two bulge PN, (a) M 2-36 (multiplied by five) and (b) M 1-42, showing the rich ORLs from C, N, O and Ne ions. The strongest transitions from the 3d–4f configuration of C II, N II, O II and Ne II are marked.

where  $\alpha_{\text{eff}}(\text{H}\beta)$  and  $\alpha_{\text{eff}}(X^{+i}, \lambda)$  are respectively the effective recombination coefficients of H $\beta$  and line  $\lambda$  emitted by ion  $X^{+i}$  following recombination. References for effective recombination coefficients currently available for C, N, O and Ne ions and a critical evaluation of their accuracy can be found in Liu et al. (2000). For a long time,  $\lambda 4267$  was the only C II ORL measured. However, it is now possible to detect fainter C II lines from higher excited levels, such as 4p–5d  $\lambda 6259$ , 4d–6f  $\lambda 6151$ , 4f–6g  $\lambda 6462$  and 4f–7g  $\lambda 5342$ , whose intensities relative to  $\lambda 4267$  are in good agreement with recombination theory (Liu et al. 2000). O II ORLs are probably the best studied so far. Peimbert et al. (1993) analyzed O II lines detected in the H II regions M 42 and M 17 and the PN NGC 6572 and found that they yield higher  $\text{O}^{2+}/\text{H}^+$  abundances than the green nebular lines. The extremely rich O II spectrum of NGC 7009 was first noticed by Wyse (1942). Using deep spectra obtained at Lick and Mount Wilson, Aller & Kaler (1964) and Kaler & Aller (1969) identified more than a hundred O II transitions. High quality IPCS and CCD spectra of NGC 7009 were obtained by Liu et al. (1995). A thorough analysis shows that, after the breakdown of *LS*-coupling for the 3p–3d and 3d–4f transitions has been accounted for, the observed relative intensities of O II lines are in excellent agreement with the predictions of recombination theory.

Similar analyses have been done in three additional objects, NGC 6153 (Liu et al. 2000), M 1-42 and M 2-36 (Liu et al. 2001b), all showing extremely rich CNONE ORLs, similar to those observed in NGC 7009, and in several less extreme PN (Liu et

al. 1999). Ne II ORLs in NGC 7009 are analyzed by Luo et al. (2001). In all cases, the observed relative intensities are in good agreement with recombination theory, thus supporting the recombination origin of these lines. The only exception are N II *triplet* lines observed in M 1-42 from the low excitation 3s–3p and 3p–3d arrays, which yield much higher  $\text{N}^{2+}/\text{H}^+$  abundances than the 3d–4f lines and the singlet lines—suggesting that the 3s–3p and 3p–3d triplet lines are fluorescence enhanced. Fluorescence excitation of N II 3s–3p and 3p–3d triplet lines was previously known to occur in Orion. Grandi (1976) suggested that they are excited by absorption of He I  $1s^2\ ^1S-1s8p\ ^1P^o\ \lambda 508.64$  which coincides in wavelength with the N II resonance line  $2p^2\ ^3P_0-2p4s\ ^3P_1^o$  at 508.67 Å, and by absorption of stellar continuum radiation. Given the faintness of the 3p–4s lines compared to the 3s–3p and 3p–3d lines, the latter mechanism probably dominates (Liu et al. 2001b).

Dinerstein et al. (2000) claim that there is a large scatter amongst  $\text{O}^{2+}/\text{H}^+$  derived from O II ORLs, and that the scatter increases with the discrepancy between the ORL and CEL abundances. No such trends are seen in our data set. Amongst NGC 7009, M 2-36, NGC 6153 and M 1-42, where the Balmer jump temperature range from 3600 to 8200 K and the ratio of ORL and CEL  $\text{O}^{2+}/\text{H}^+$  abundances varies from 5 to 20, the intensities of O II lines relative to 3d–4f  $\lambda 4089$  are found to be remarkably uniform, and vary by only  $\sim 20\%$  in the case of the 3p and 3d lines, and a factor of 1.6 for those arising from the 3p' and 3d' doubly excited levels.

The small variations as a function of Balmer jump temperature agree with the expectations of recombination theory (Liu et al. 2001b). The comparison of ionic abundance ratios derived from CELs and ORLs involves comparing lines whose intensities differ by over three orders of magnitude. To ensure that no systematic errors occur for measurements over such a large dynamical range, Mathis & Liu (1999) measured the  $[\text{O III}] \lambda 4931/\lambda 4959$  ratios in a number of PN. Since both lines arise from the same upper level, so their intensity ratio is independent of all physical conditions. The fainter  $\lambda 4931$  line has an intensity comparable to O II ORLs. They find  $10^4 \times \lambda 4931/\lambda 4959 = 4.15 \pm 0.11$ , compared to theoretical values of 4.09 (Nussbaumer & Storey 1981), 4.15 (Froese Fisher & Saha 1985) and 2.50 (Galavis et al. 1997).

The main conclusions from our detailed abundance analyses that have been carried out in a number of PNe, using both the ORL and CEL methods and utilizing observational data from the UV to far-IR, are as follows (cf. also Liu et al. 1999):

1. It is now possible to obtain high quality measurements for many faint nebular emission lines, down to intensities of  $\sim 10^{-4}$  of  $H\beta$ . The observed relative intensities of C II, N II, O II and Ne II permitted transitions are in good agreement with the predictions of recombination theory, thus confirming their recombination origin.
2. For all the ionic species studied so far, including  $\text{C}^{2+}$ ,  $\text{N}^{2+}$ ,  $\text{O}^{2+}$  and  $\text{Ne}^{2+}$ , the ionic abundances relative to  $\text{H}^+$  derived from ORLs are invariably higher than the corresponding values deduced from CELs – UV, optical and infrared, regardless of the excitation energy or the critical density of the CELs. The discrepancy varies from target to target and covers a wide range from unity (i.e. near agreement) to over a factor of twenty. However, discrepancies over a factor of five are rare, and are found only in a small number of PN (about 5%). For most nebulae, the discrepancies are about a factor of two.
3. For a given nebula, the discrepancies for C, N, O and Ne, are found to be approximately the same magnitude, a result which may have a fundamental implication for the underlying cause(s) of the discrepancies. It also implies that, while the absolute heavy element abundances relative to H remain uncertain, the relative abundances of heavy elements (such as C/O, N/O and Ne/O) are probably secure, provided that the

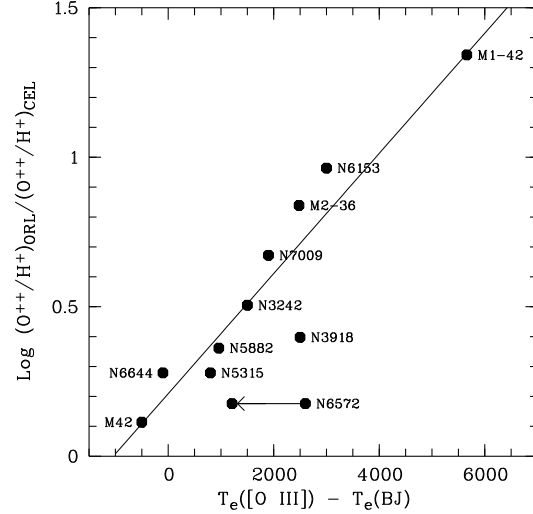


Fig. 2. The logarithm of the ratio of  $\text{O}^{2+}/\text{H}^+$  derived from O II ORLs and from  $[\text{O III}]$  CELs is plotted against the difference between the  $[\text{O III}]$  forbidden line and Balmer jump temperatures. The solid line is a linear fit to  $\Delta(\text{O}^{2+}/\text{H}^+) \equiv \log(\text{O}^{2+}/\text{H}^+)_{\text{ORL}} - \log(\text{O}^{2+}/\text{H}^+)_{\text{CEL}}$  as a function of  $\Delta T \equiv T_e([\text{O III}]) - T_e(\text{BJ})$ .

same type of emission lines, ORLs or CELs, are used to determine heavy element abundances involved in the ratios.

4. Observational uncertainties, fluorescence excitation or blending with unknown lines as the cause of discrepancies can be ruled out.

### 3. CAUSES OF ABUNDANCE DISCREPANCIES

The determinations of ORL abundances for a number of heavy elements, each derived from a large number of transitions, and comparing CEL abundances deduced from lines of different characteristics, such as excitation energy and critical density, place strong constraints on the possible physical cause(s) of the discrepancies between the heavy element abundances derived from these two types of emission lines. For the first time, it is now possible to examine *quantitatively* the existence and magnitude of the long-debated temperature, density and chemical inhomogeneities and their effects on nebular abundance determinations.

#### 3.1. Temperature fluctuations

Evidence pointing to the presence of large temperature fluctuations in PN was first given by Peimbert (1967, 1971), who found that electron temperatures derived from the Balmer jump are systematically lower than those derived from the  $[\text{O III}]$  forbidden line ratio. This was confirmed by Liu & Danziger

(1993b) who compared the Balmer jump and [O III] temperatures for a large sample of PNe, including those measured previously by Barker (1978). On average,  $t^2 \sim 0.035$ , or fluctuations with an amplitude of 20%, enough to cause the  $\lambda\lambda 4959, 5007$  forbidden line  $O^{2+}/H^+$  abundance ratio to be underestimated by a factor of two. In M1-42 where  $O^{2+}/H^+$  derived from ORLs is twenty times higher than that yielded by CELs, we measured a record low  $T_e(\text{BJ})$  of 3560 K, compared to  $T_e([\text{O III}]) = 9220$  K (Liu et al. 2001b). A spatial analysis of NGC 6153 along its minor-axis shows that the difference between  $T_e([\text{O III}])$  and  $T_e(\text{BJ})$  decreases with nebular radius, so does the ratio of the ORL and CEL  $O^{2+}/H^+$  abundances. Previous analyses of several large PN by Barker also found that the ratio of  $C^{2+}/H^+$  derived from C II  $\lambda 4267$  and from C III]  $\lambda 1908$  decreases with distance from the nebular centre (Barker 1987 and references therein). With data now available, the possibilities of fluorescence excitation or blending with unknown lines of  $\lambda 4267$  as the cause, as previously suspected, can be ruled out. Figure 2, taken from Liu et al. (2001b), shows that the ratio of ORL and CEL abundances correlates with the difference between [O III] forbidden line and Balmer jump temperatures. The tight correlation provides the strongest evidence so far that the two phenomena, i.e. the disparity between electron temperatures deduced from the two  $T_e$ -diagnostics, and the disparity between heavy element abundances derived from the two types of emission lines, are closely related and probably have the same physical origin.

Dinerstein et al. (1985) derived  $T_e$  for four PN using the [O III]  $\lambda 5007/52 \mu\text{m}$  ratio and found that they are systematically lower than those yielded by the optical  $\lambda 4363/\lambda 5007$  ratio, suggesting large temperature fluctuations. However, a reanalysis of the NGC 6543 KAO data by Dinerstein et al. (1995) yields  $t^2 \sim 0$ . This method of  $t^2$  determination has the advantage that only lines from the same ion are involved. However, given the very low critical density of the  $52 \mu\text{m}$  line, the  $\lambda 5007/52 \mu\text{m}$  temperature can easily be overestimated for nebulae with modest density inhomogeneities, thus offsetting the effects of temperature fluctuations. [Ne III]  $15.5 \mu\text{m}$  and [Ar III]  $9.0 \mu\text{m}$  have a much higher critical density than the  $52 \mu\text{m}$  line. Thus comparing  $T_e$ 's derived from the [Ne III]  $\lambda 3868/15.5 \mu\text{m}$  and  $\lambda 3342/\lambda 3868$  diagnostic pair or from the [Ar III]  $\lambda 7135/9.0 \mu\text{m}$  and  $\lambda 5193/\lambda 7135$  pair could be more useful.

For M1-42,  $T_e(\text{BJ})$  is more than a factor of 2 lower than  $T_e([\text{O III}])$ . For such an extreme object, the concept of temperature fluctuations as envisaged

originally by Peimbert (1967) is probably no longer applicable. For other less extreme nebulae, the  $t^2$  derived from  $T_e(\text{BJ})$  and  $T_e([\text{O III}])$  is often found to be too small to explain the difference between the ORL and CEL abundances. Most importantly, temperature fluctuations are unable to explain the low abundances derived from the  $T_e$ -insensitive IR fine-structure lines. For all nebulae studied so far, IR fine-structure lines yield ionic abundances comparable to or only slightly higher than those derived from optical or UV CELs, but much lower than the values implied by ORLs (Rubin et al. 1997; Liu et al. 2000; 2001a,b). Clearly, something in addition to temperature fluctuations is needed to explain the large disparity between the ORL and CEL abundances.

### 3.2. Density condensations

High resolution *HST* images now available for many PN demonstrate that PN are far from homogeneous Strömgren spheres of ionized gas. Instead, loops, filaments and knots colliding with fast winds from the central star, are ubiquitous. The WFPC2 images of NGC 6153 taken in  $H\alpha$  and [O III]  $\lambda 5007$  filters reveal nearly identical honeycomb structures, suggesting they consist of ionized high-density material. Analyses of *ISO* LWS spectra for a large sample of PN show that  $N_e$ 's derived from the [O III]  $88\mu\text{m}/52\mu\text{m}$  ratio are systematically lower than those yielded by the optical [Ar IV] and [Cl III] doublet ratios, pointing to the presence of high density regions in the nebula, where the 52- and  $88 \mu\text{m}$  lines are suppressed by collisional de-excitation due to their low critical densities (Liu 1997; Liu et al. 2001a). Apart from the general effect of reducing the emissivities of CELs relative to  $H\beta$  (Rubin 1989), condensations with  $N_e \gtrsim 10^6 \text{cm}^{-3}$  suppress the  $\lambda\lambda 4959, 5007$  lines relative to the  $\lambda 4363$  line, leading to an artificially high [O III] temperature (Viegas & Clegg 1994). Overestimated temperatures can have a profound effect on ionic abundances derived from CELs with a high excitation energy.

However, Balmer decrement analyses show that there is no substantial amount of gas in such high density condensations. In NGC 6153, M1-42 and M2-36, the Balmer decrement yields  $N_e \sim$  a few  $\times 10^3 \text{cm}^{-3}$ , comparable to values derived from optical forbidden line ratios, and only moderately higher than those deduced from the  $88 \mu\text{m}/52 \mu\text{m}$  ratio. With a critical density of  $2 \times 10^5 \text{cm}^{-3}$ , the [Ne III]  $15.5 \mu\text{m}$  line is particularly difficult to suppress.

### 3.3. Chemical inhomogeneities

Torres-Peimbert et al. (1990) show that by assuming an inner C-rich zone in NGC 4361, the

large discrepancy between the C abundances deduced from ORLs and CELs can be reconciled. Deep long-slit spectroscopy however found no evidence of a carbon abundance gradient across this nebula (Liu 1998). On the other hand, a steady decrease of C and O abundances from the nebular centre is observed in NGC 6153. A weak O VI emission line at 3811 Å is also detected in the central star spectrum of NGC 6153, suggesting the nucleus has a H-deficient surface. We find that empirical nebular models containing two components, each with its own temperature, density and chemical composition, are able to account for many of the observed patterns in NGC 6153 (Liu et al. 2000). One such model, which gives a good fit to the observed line intensities, has 500 K H-depleted material, presumed to be evaporating from dense neutral inclusions, embedded in 9500 K material with ‘normal’ abundances. An alternative model, which appears more physically plausible on a number of grounds, has high-density ( $2 \times 10^6 \text{ cm}^{-3}$ ), fully ionized, H-deficient knots embedded in the ‘normal’ component. In both models, the metal-rich component has a He/H abundance ratio of 0.3–0.4 and an O/H ratio which is  $\sim 100$  times higher than that of the diffuse gas. A detailed photoionization model of NGC 6153, incorporating H-deficient inclusions (Péquignot, this volume). A small number of PN with H-deficient knots embedded in a nebula with a ‘normal’ metallicity are already known to exist, including the archetypes Abell 30 and Abell 78 (Jacoby & Ford 1983), and are interpreted by Iben et al. (1983) as “born-again” PN. We have recently obtained deep optical spectra of knots J1 and J3 in A 30. All the strongest ORLs observed in NGC 6153 and M 1-42 are also prominent in these spectra, including lines from C II, C III, N II, N III, O II and Ne II, consistent with the high metallicity nature of these knots. High spatial resolution *HST* STIS observations are also planned. Analysis of these data should provide us with a much better understanding of the physics of H-deficient knots—their thermal, density and ionization structure and their effects on abundance determinations.

## REFERENCES

- Aller, L. H., & Kaler, J. B. 1964, *ApJ*, 139, 1074  
 Aller, L. H., & Menzel, D. H., 1945 *ApJ*, 102, 239  
 Barker, T. 1978, *ApJ*, 219, 914  
 ———. 1987, *ApJ*, 322, 922  
 ———. 1991, *ApJ*, 371, 217  
 Burgess, A., & Seaton, M. J. 1960, *MNRAS*, 121, 76  
 Cunto, W., Mendoza, C., Ochsenbein, F., & Zeippen, C. J. 1993, *A&A*, 275, L5  
 Dalgarno, A., Heil, T. G., & Butler, S. E., 1981, *ApJ*, 245, 793  
 Dinerstein, H. L., Haas, M. R., Erickson, E. F., & Werner, M. W. 1995, in *Galactic Ecosystem*, ed M. R. Haas, et al. (San Francisco: ASP), 387  
 Dinerstein, H. L., Lafon, C. E., & Garnett, D. R. 2000, in *ASP Conference Series Vol. 199, Asymmetrical Planetary Nebulae II: From Origins to Microstructures*, eds. J. H. Kastner, N. Soker, & S. Rappaport (San Francisco: ASP), 301  
 Dinerstein, H. L., Lester, D., & Werner, M. W. 1985, *ApJ*, 291, 561  
 Galavis, M. E., Mendoza, C., & Zeippen, C. J. 1997, *A&AS*, 123, 159  
 Froese Fisher, C., & Saha, H. P. 1985, *Phys. Scri.*, 32, 181  
 Grandi, S. A. 1975, *ApJ*, 196, 465  
 ———. 1976, *ApJ*, 206, 658  
 Harrington, J. P., Lutz, J. H., Seaton, M. J., & Stickland, D. J. 1980, *MNRAS*, 191, 13  
 Iben, I., Jr., Kaler, J. B., Truran, J. W., & Renzini, A. 1983, *ApJ*, 264, 605  
 Jacoby, G. H., & Ford, H. C. 1983, *ApJ*, 266, 298  
 Kaler, J. B. 1972, *ApJ*, 173, 601  
 ———. 1986, *ApJ*, 308, 337  
 Kaler, J. B., & Aller, L. H. 1969, *ApJ*, 157, 1231  
 Liu, X.-W. 1997, in *Analytical Spectroscopy*, ed. M. F. Kessler, ESA Publ., ESTEC, 87  
 Liu X.-W. 1998, *MNRAS*, 295, 699  
 Liu, X.-W., Barlow, M. J., Danziger, I. J., & Storey, P. J., 1999, in *Chemical Evolution from Zero to High Redshift*, eds. Walsh, J. R., Rosa, M. R. (Berlin: Springer-Verlag), 39  
 Liu, X.-W., Danziger, I. J. 1993a, *MNRAS*, 261, 465  
 ———. 1993b, *MNRAS*, 263, 256  
 Liu, X.-W., Luo, S.-G., Barlow, M. J., Danziger, I. J., & Storey, P. J., 2001b, *MNRAS*, 327, 141  
 Liu, X.-W., Storey, P. J., Barlow, M. J., & Clegg, R. E. S., 1995, *MNRAS*, 272, 369  
 Liu, X.-W., Storey, P. J., Barlow, M. J., Danziger, I. J., Cohen, M., & Bryce, M. 2000, *MNRAS*, 312, 585  
 Liu, X.-W., et al., 2001a, *MNRAS*, 323, 343  
 Luo, S.-G., Liu, X.-W., Barlow, M. J., 2001, *MNRAS*, 326, 1049  
 Mathis, J. S., & Liu, X.-W. 1999, *ApJ*, 521, 212  
 Menzel, D. H., & Aller, L. H. 1941, *ApJ*, 94, 30  
 Miller, J. S. 1971, *ApJ*, 165, L101  
 Nussbaumer, H., & Storey, P. J. 1981, *A&A*, 99, 177  
 Peimbert, M. 1967, *ApJ*, 150, 825  
 ———. 1971, *Bol. Obs. Ton. Tac.*, 6, 29  
 ———. 1994, in *The Analysis of Emission Lines*, eds. Williams R., Livio M. (Cambridge, UK: CUP), 165  
 Peimbert, M., Storey, P. J., & Torres-Peimbert, S. 1993, *ApJ*, 414, 626  
 Rola, C., & Stasińska G. 1994, *A&A*, 282, 199  
 Rubin, R. H. 1989, *ApJS*, 69, 897  
 Rubin, R. H., Colgan, S. W. J., Haas, M. R., Lord, S., & Simpson, J. P. 1997, *ApJ*, 479, 332

Seaton, M. J. 1968, MNRAS, 139, 129

\_\_\_\_\_. 1987, J. Phys. B, 20, 6363

Stasińska G. 1998, in Abundance Profiles: Diagnostic Tools for Galaxy History, eds. Friedli, D., et al. (San Francisco: ASP), 142

Storey, P. J. 1994, MNRAS, 282, 999

Torres-Peimbert, S., & Peimbert, M. 1977, RevMexAA, 2, 181

Torres-Peimbert, S., Peimbert, M., & Peña, M. 1990, A&A, 233, 540

Viegas, S., & Clegg, R. E. S. 1994, MNRAS, 271, 993

Wyse, A. B. 1942, ApJ, 95, 356



Xiao-Wei Liu, Siek Hyung, & Daniel Péquignot

X.-W. Liu: Department of Physics and Astronomy, University College London, Gower Street, London WC1E 6BT, UK (xwl@star.ucl.ac.uk).